Palaeogeography, Palaeoclimatology, Palaeoecology 685 (2026) 113547

Contents lists available at ScienceDirect

Palaeogeography, Palaeoclimatology, Palaeoecology

journal homepage: www.elsevier.com/locate/palaeo

Middle Eocene hyperthermal seasonality from Paris Basin marine mollusks

Loïc Marlot [a,b,c], Damien Huyghe [a,*], Justine Briais [b], Mathieu Daëron [d], Christine Flehoc [b], Laurent Emmanuel [e], Didier Merle [f], Olivier Aguerre-Chariol [g], Franck Lartaud [h]

[a] PSL University/MINES Paris, Centre de Géosciences, 35 rue St Honoré, F-77305 Fontainebleau, France
[b] BRGM (French Geological Survey), F-45060 Orléans Cedex 2, France
[c] Now at IMT Nord Europe, Institut Mines-Télécom, Lille University, Centre for Energy and Environment, Lille F-59000, France
[d] Laboratoire des Sciences du Climat et de l'Environnement, LSCE/IPSL, CEA-CNRS-UVSQ, Université Paris-Saclay, Bât 714, CEA-Orme des merisiers, RD 128 F-91191 GIF-SUR-YVETTE CEDEX, France
[e] Sorbonne Université, UMR CNRS 7193, Institut des Sciences de la Terre de Paris, ISTeP, 4 place Jussieu, F-75005 Paris, France
[f] Muséum National d'histoire Naturelle, Département Origines et Évolution (CR2P - MNHN, CNRS, UPMC, Sorbonne Université), 8 rue Buffon, F-75005 Paris, France
[g] Independant, 14 rue Saint-Hubert, 60560 Orry-la-Ville
[h] Sorbonne Université, CNRS, Laboratoire d'Écogéochimie des Environnements Benthiques (LECOB), Observatoire Océanologique de Banyuls, F-66650, Banyuls-sur-mer, France

ARTICLE INFO

Editor: Bing Shen

Keywords:
Climate change
Mollusk
Middle Eocene climatic optimum
Stable isotopes
Clumped isotopes

ABSTRACT

The Earth has experienced hyperthermal events in the past, characterized by maximum durations of hundreds thousand years, significant magnitude, global extent, and drivers associated with increases in greenhouse gas concentrations, therefore making them potential analogues for current climate change. The Middle Eocene Climatic Optimum (MECO) that occurred 40 Ma ago, is marked by a CO_2-driven global warming of +4 to +6 °C, affecting global temperatures. Here, we present a detailed reconstruction of seasonal fluctuations in seawater temperatures during this warming event in littoral environment, based on geochemical analyses ($\delta^{18}O$ and Δ_{47}) of shallow-marine mollusks from the Paris Basin. Our data show a stability in mean winter temperatures compared to pre-MECO conditions, but a marked warming of +10 °C in maximum estuarine water temperatures, with a seasonal temperature range increasing from 12 °C before the MECO to 22 °C at the climax of the event. We demonstrate that at mid-latitudes, annual maximum shallow-water temperatures increased from 30 ± 2 °C before the event to a maximum of 41 ± 4 °C at the warming peak. This pattern is associated with a seasonal regime characterized by dry summers and wet winters, implying that the Paris Basin experienced a super-hot summer Mediterranean climate during the MECO.

1. Introduction

Modern anthropogenic greenhouse gases emissions are driving a rapid increase in global temperatures, unprecedented in the historical record. The 2023 Intergovernmental Panel on Climate Change (IPCC) report proposed different scenarios of climate evolution, leading to a return to paleoclimatic conditions observed during the Pliocene, the Early Eocene or even the Late Cretaceous under the most pessimistic scenario (Burke et al., 2018; Tierney et al., 2020). Although no exact analogue exists for the ongoing climate change, studying past episodes of global warming driven by increasing atmospheric greenhouse gas concentrations, can provide valuable insights for better understanding and characterizing future climate conditions (Lear et al., 2021; Tierney et al., 2020).

After the Early Eocene Climatic Optimum, the Earth entered a long-term cooling trend punctuated by several short-term warming events (Westerhold et al., 2020; Zachos et al., 2001). The Middle Eocene Climatic Optimum (MECO), occurring between 40.5 and 40 million years ago (Bohaty et al., 2009; Westerhold et al., 2020), is marked by a rise in both deep-sea and sea-surface temperatures (SST) of 4–6 °C in ~500 ky (Bohaty and Zachos, 2003: Bohaty et al., 2009; Cramwinckel et al., 2018). In contrast to other Early Paleogene hyperthermals that are commonly linked to CH_4 emissions, such as the Paleocene-Eocene Thermal Maximum (PETM), the MECO is interpreted as the only global warming event primarily driven by elevated atmospheric CO_2 levels (Bohaty and Zachos, 2003; Henehan et al., 2020; Sluijs et al.,

* Corresponding author.
E-mail address: damien.huyghe@minesparis.psl.eu (D. Huyghe).

https://doi.org/10.1016/j.palaeo.2026.113547
Received 29 August 2025; Received in revised form 19 December 2025; Accepted 3 January 2026
Available online 5 January 2026

2013). The short duration, the magnitude and global impact of the warming, the associated sea level rise (Bohaty et al., 2009; Brachert et al., 2023; Henehan et al., 2020) and resulting biodiversity changes (Bijl et al., 2011; Boscolo Galazzo et al., 2015; Edgar et al., 2013), makes the MECO one of the most compelling paleoclimate analogues for the ongoing global climatic change (Sluijs et al., 2013).

The climatic history of this warming is now well-documented in the oceanic domain, mostly through geochemical analyses of deep-sea benthic and planktonic foraminifera (Bijl et al., 2010; Bohaty et al., 2009; Bohaty and Zachos, 2003; Cramwinckel et al., 2018; Westerhold et al., 2020). However, these proxies provide reconstructions of mean annual temperatures, leaving key climatic components, such as seasonal temperature variations, poorly understood. Characterizing paleotemperature reconstructions at the seasonal scale is however essential to capture short-term climatic dynamics and to better constrain the mechanisms driving environmental variability (De Winter et al., 2024; He et al., 2025; Ivany and Judd, 2022). Such fine-scale reconstructions provide valuable information about seasonality shifts, extreme events, and their ecological impacts factors often obscured in lower-resolution records. Advancing this level of characterization therefore enhances the accuracy of climate models and improves our ability to interpret the sensitivity of past and future climate systems.

In this study, we aim to identify and characterize seasonal temperature fluctuations, before, during and after the MECO. To achieve this, we target on shallow-marine environments that hosted mollusk shells, which allow seasonal-scale temperatures reconstructions through high-resolution stable isotope analyses of their growth bands (Andreasson and Schmitz, 1996; Huyghe et al., 2022; Kniest et al., 2024; De Winter et al., 2020).

2. Geological setting

This work focuses on the Paris Basin, which provides a unique record of middle Eocene sediments, with the preservation of coastal deposits that hosted a biodiversity hotspot for shallow-marine ecosystems during the Middle Eocene (Huyghe et al., 2012a; Merle, 2008), allowing for reliable high-resolution paleoclimatic reconstructions.

The Paris Basin is a well-known intracratonic sedimentary basin that underwent long-term subsidence during the Mesozoic, with a period of negligible subsidence during the Paleogene, followed by regional uplift during the Neogene (Cavelier and Pomerol, 1979; Guillocheau et al., 2000; Robin et al., 2003). During the Eocene, the basin extended northward to include the Hampshire and Brussels basins (Pomerol, 1973) and was connected to both the North Sea and the Atlantic Ocean via the English Channel (Fig. 1; Gély and Lorenz, 1991).

Until the end of the Middle Lutetian, marine inflow was primarily from the North Sea. Following the uplift of the Artois and Bray anticlines, inflow became exclusively of North Atlantic origin (Pomerol, 1973; Gély and Lorenz, 1991). Low paleotopographic relief and negligible subsidence during the Paleogene meant sediment distribution was predominantly controlled by eustatic sea-level fluctuations (Mégnien, 1980; Briais, 2015), modulated by tectonic reactivation of anticlines, resulting in significant lateral facies variations complicating basin-wide stratigraphic correlations (Briais, 2015; Gély and Lorenz, 1991; Moreau et al., 2024).

During the Middle Eocene, most shallow-water sedimentary deposits were located in the northern part of the Paris basin. In the Middle Lutetian, sedimentation was dominated by carbonate platform deposits, particularly the Calcaire Grossier Formation. From the Late Lutetian to the Early Bartonian, sedimentation shifted toward lagoonal facies with intense evaporation, leading to the deposition of the Marnes et Caillasses Formation (Briais, 2015; Moreau et al., 2024).

The Bartonian stratigraphy comprises two regional stages: the Auversian, beginning with the Marnes et Caillasses Formation, and followed by siliciclastic shallow-marine deposits, including the Sables d'Auvers and Sables de Beauchamp Formations (Pomerol, 1965). Then the Marinesian local stage, corresponding to the Late Bartonian, is characterized by lagoonal to lagoon-lacustrine calcareous sedimentation (Briais, 2015; Morellet and Morellet, 1948).

This succession of shallow-marine environments enables detailed climatic reconstructions in littoral settings throughout the Middle Eocene, due to exceptionally well-preserved and diverse faunal assemblages in the basin during this period (> 800 species in the Early Bartonian, and >1400 species during the peak of marine biodiversity at the Middle Lutetian; Merle, 2008).

3. Materials and methods

3.1. Field Sampling

Fossils analyzed in this study were collected north of Paris, from sites near Chavençon, Chars, and the protected geological site of Le Guépelle, recently described by Aguerre-Chariol (2023) (Fig. 1). Sampling was conducted in sandy layers where fossil shells were well-preserved and easily extractable, allowing access to whole specimens.

To minimize uncertainties related to species-specific isotopic fractionation, we sampled the most abundant mollusk families present at each site. Thus, we sampled gastropod shells of the species *Torquesia sulcifera* (Deshayes, 1832) (Turritellidae) from the Horizon de Mont Saint-Martin (HMSM) in Chavençon (Turritellidae), and the bivalves

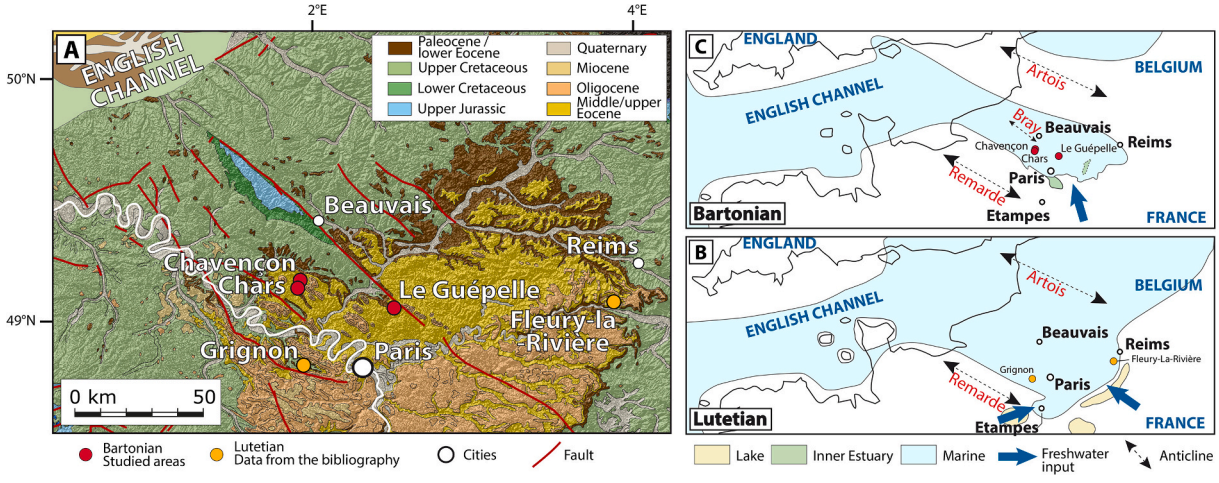

Fig. 1. A: Geological map of the Paris Basin and location of the sampling sites. For the Lutetian sites, data are from Andreasson and Schmitz (1996); Huyghe et al. (2012b) and De Winter et al. (2020). B: Paleogeographic map of the Paris Basin during the Lutetian (Merle, 2008) and C: during the Bartonian (Briais, 2015).

Bicorbula gallica (Lamarck, 1801) (Corbulidae) from the site of Le Guépelle and *Orthocardium porulosum* (Solander, 1766) (Cardiidae) from the Sables de Cresnes Fm in Chars (Fig. 2). Two or three specimens were sampled per stratigraphic level, except at the uppermost level (Sables de Cresnes Fm.), where only one large sample was available.

3.2. Studied taxa

The Turritellidae analyzed in this study include the Bartonian species *Torquesia sulcifera* (Deshayes, 1832). These large gastropods (~10 cm) possess aragonitic shells and are morphologically comparable to extant members of the genus *Turritella*. Turritellidae are commonly used in paleoclimatic reconstructions due to their capacity to record multi-annual seasonal climate variations within their shell growth, and their typically large size allows for high-resolution sampling (Andreasson and Schmitz, 2000; Andreasson and Schmitz, 1996; Huyghe et al., 2012a; Marchegiano and John, 2022). Additionally, modern representatives of this family exhibit a low tolerance to salinity fluctuations (Allmon, 1988), making them reliable indicators of stable marine conditions in paleoenvironmental studies.

The Corbulidae are represented by *Bicorbula gallica*, collected from Le Guépelle section (Fig. 4). Members of the Corbulidae family are typically filter feeders and surface deposit scrapers that inhabit intertidal to shallow subtidal environments (Holmes and Miller, 2006; Mirzaei and Hosseini, 2017). Modern corbulids are widespread in shallow marine waters, ranging from the Norwegian Sea to the western coast of Africa (Fuksi et al., 2018; Holmes and Miller, 2006). They are well adapted to warm temperatures and can tolerate hypoxic conditions as well as significant salinity fluctuations (Fuksi et al., 2018; Holmes and Miller, 2006).

The third species correspond to the bivalve *Orthocardium porulosum*, with only one specimen from the Sables de Cresnes formation at Chars. The Cardiidae family comprises shallow-marine endobenthic species.

3.3. Preservation screening

To ensure that the stable isotope composition of biogenic carbonates reliably reflects paleoenvironmental conditions, it is essential that the mollusk shells used in this study are free from diagenetic alteration. Preservation was assessed using cathodoluminescence microscopy to test the good preservation of growth increments (greenish luminescence indicating preserved aragonite; Barbin, 2013; de Rafélis et al., 2000) and X-ray diffraction (XRD) analyses was conducted on powdered shell material, confirming exclusive aragonite preservation with no detectable secondary phases (Supplementary Material 1). Bivalves of the species *Bicorbulla gallica* show very low but homogenous luminescence. Gastropods are on the contrary completely non-luminescent (totally dark) under CL attesting non recrystallisation of secondary calcite and preservation of their primary aragonitic mineralogy.

3.4. Sample preparation and micromilling

After collection, sediment samples were sieved and sorted to isolate complete shells suitable for isotopic analyses. Each shell underwent a standardized cleaning protocol following the method described by (Lartaud et al., 2010). Initially, the shells were rinsed with distilled water, then immersed in a 6 % H_2O_2 solution for six hours to eliminate residual organic matter. This was followed by a 20-min bath in 0.15 N HNO_3 to remove any external recrystallized calcite.

Isotopic sampling was performed using conventional micromilling techniques, with sampling along the growth axis using a 0.1 mm drill bit (Huyghe et al., 2015; De Winter et al., 2020). Multiple samples were extracted from each shell to capture seasonal variations in isotopic composition ($\delta^{18}O$ and Δ_{47}).

3.5. Stable Isotope analyses

Each shell was analyzed for $\delta^{18}O$ composition. All stable isotope values are presented in Supplementary Material 2. After micromilling, $\delta^{18}O$ analyses were performed on 50 to 100 µg carbonate powder samples, reacted with 100 % phosphoric acid (H_3PO_4) at 90 °C under vacuum. The resulting CO_2 was ionized and measured using an Isoprime 100 dual-inlet mass spectrometer. Results are reported in delta (δ) notation relative to the Vienna Pee Dee Belemnite standard (‰ VPDB) with ±0.2 ‰ precision (1σ), using CO-1 (for oxygen), NBS-19 (for combined carbon-oxygen calibration), and an internal Carrara marble (calibrated

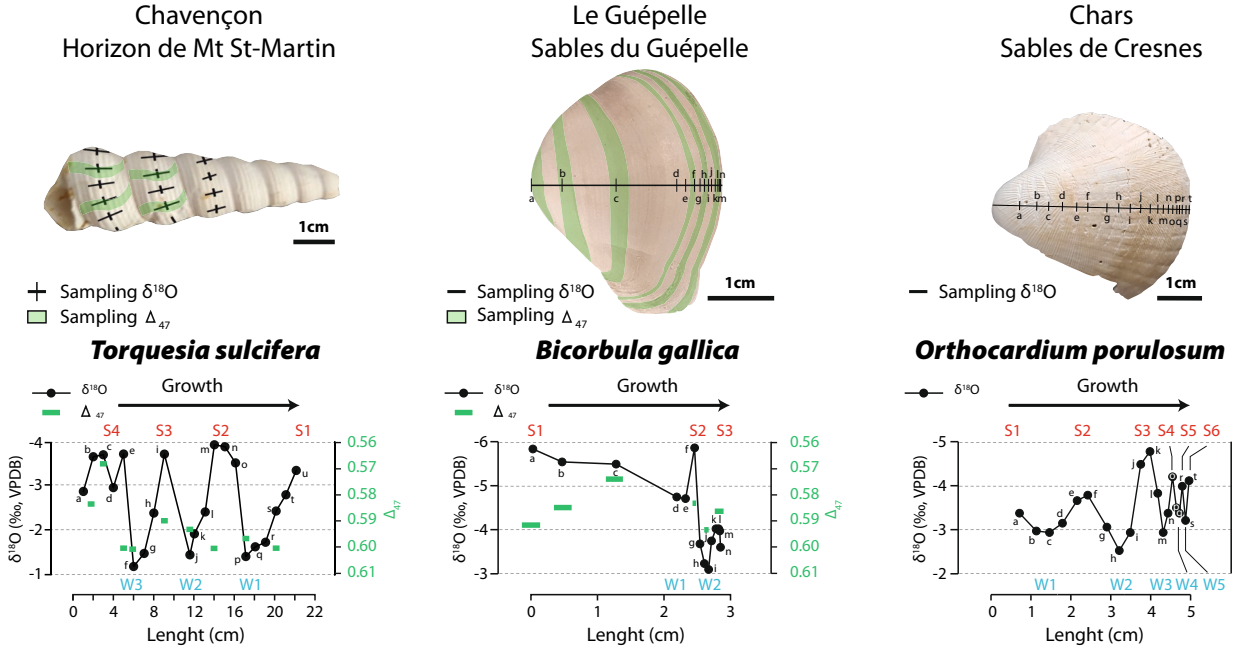

Fig. 2. Mollusk species analyzed in this work: *Torquesia sulcifera*, *Bicorbula gallica* and *Orthocardium porulosum*. The area of the shell sampled for both $\delta^{18}O$ and Δ_{47} analyses is illustrated on each shell. The corresponding isotopic signal and the identification of each summer (S) and winter period (W) on a given shell is reported for each shell.

against CO-1) as standards.

Clumped isotope (Δ_{47}) analyses were performed on two *T. sulcifera* shells from the HMSM and two *B. gallica* shells from the base and top of the Sables du Guépelle Formation, corresponding to the Modiolaria zone, the Ermenonville Formation, and the Sables de Beauchamp Formations. These analyses were conducted at the Laboratoire des Sciences du Climat et de l'Environnement (LSCE) using protocols and instrumentation described in (Daëron et al., 2019; Peral et al., 2018) and in the attached analytical report (Supplementary Material 3).

For each analysis, 4 mg of sample powder were dissolved in 100 % H_3PO acid at 90 °C for 15 min. The resulting CO_2 was then quantitatively recollected by cryogenic trapping and transferred by gas expansion into an Isoprime 100 dual-inlet mass spectrometer equipped with six Faraday collectors (*m/z* 44 to 49). (δ 45 to δ 49) were converted to $\delta^{13}C$, $\delta^{18}O$, and "raw" Δ_{47} values as described by (Daëron et al., 2016) using the IUPAC oxygen- 17 correction parameters (Brand et al., 2010). The isotopic composition ($\delta^{13}C$, $\delta^{18}O$) of our working reference gas was computed based on the nominal isotopic composition of all ETH carbonate standards (Bernasconi et al., 2018) and an oxygen-18 acid fractionation factor of 1.00813. Raw Δ_{47} values were then converted to the I-CDES (InterCarb-Carbon Dioxide Equilibrium Scale) reference frame (Bernasconi et al., 2021) using a pooled regression approach (Daëron, 2021) as implemented by the D47crunch Python library. Full analytical errors are derived from the external reproducibility of unknowns and standards (Nf = 29) and conservatively account for the uncertainties in raw Δ_{47} measurements as well as those associated with the conversion to the I-CDES reference frame (Daëron, 2021). Seawater $\delta^{18}O_w$ was calculated using the formula of Grossman and Ku (1986). The details of the protocol and results for clumped isotopes analyses are provided in Supplementary Material 3.

3.6. Paleotemperature calculation

The primary objective of this study was to estimate paleotemperatures in littoral environments based on $\delta^{18}O$ measurements from mollusk shells. Mollusks are assumed to precipitate their shells in near isotopic equilibrium with ambient seawater (Wefer and Berger, 1991; Grossman and Ku, 1986; Quizon et al., 2025; Schlidt et al., 2025). However, cases of isotopic disequilibrium have been identified for some species, such as deep-sea oysters of the genius *Pycnodonte* (Wisshak et al., 2009) or the juvenile portion of the oysters *Maganalla gigas* (Huyghe et al., 2022). Among the fossil used in this study, specimens of the genius *Turritella* have often been employed for (paleo)climatic reconstructions (Andreasson and Schmitz, 1996; Huyghe et al., 2012b; Jones and Allmon, 1995; Scholz et al., 2020). Studies on modern specimens have shown that these gastropods mineralize their shells in equilibrium with seawater, making it possible to reconstruct seasonal temperature gradients when $\delta^{18}O_w$ is well constrained (Scholz et al., 2024). Concerning the bivalves *B. gallica* and *O. porulosum*, these species have not yet been used for paleoclimatic reconstructions. Moreover, for many mollusks, significant variations in growth rate have been documented, especially during winter periods (De Winter et al., 2020; Ivany and Judd, 2022). This requires very high-resolution sampling to ensure that true seasonal extrema are captured in stable isotopes analyses.

These environmental and biological considerations support the combined use of $\delta^{18}O$ and Δ_{47} measurements to reliably estimate $\delta^{18}O_w$ and thus the true temperature extrema. Thus, temperature can be calculated using the aragonite-specific paleotemperature equation from (Grossman and Ku, 1986) (Eq. (1)):

$$T(^{\circ}C) = 20.6 - 4.34\left(\delta^{18}O_{aragonite} - \delta^{18}O_w\right) \quad (1)$$

where T is the temperature of shell mineralization, $\delta^{18}O_{aragonite}$ is the stable oxygen isotope composition of the shell, and $\delta^{18}O_w$ is that of ambient water.

The main source of uncertainty in this calculation lies in determining $\delta^{18}O_w$. To address this, clumped isotope (Δ_{47}) analyses were conducted on the same mollusk shells, as this proxy is solely temperature-dependent (Eiler, 2011; Quizon et al., 2025; Schlidt et al., 2025). To convert Δ_{47} values into calcification temperatures, we used the composite OGLS23 calibration which combines >100 biogenic, inorganic and synthetic samples analyzed in 5 different laboratories and reprocessed in the I-CDES reference frame (Daëron and Vermeesch, 2024):

$$\Delta_{47}(^{\circ}C) = 0.1744 - \frac{18.14}{T} + \frac{42.66\,X\,10^3}{T^2} \quad (2)$$

Although this Δ_{47}–temperature calibration is largely based on calcitic foraminifera, whereas the samples analyzed in this study are aragonitic, experimental and empirical studies indicate that equilibrium Δ_{47} values do not exhibit a resolvable dependence on carbonate mineralogy, in contrast to $\delta^{18}O$ measurements, which are mineral-specific (e.g., Bonifacie et al., 2017; De Winter et al., 2022). To date, no statistically significant offset in equilibrium Δ_{47} has been demonstrated between calcite and aragonite. Consequently, Δ_{47}-based paleotemperature reconstructions from aragonitic archives, including mollusk shells, commonly rely on unified equilibrium calibrations rather than mineral-specific equations. Within the I-CDES framework, this approach can be considered appropriate for reconstructing temperatures from the aragonitic mollusk shells analyzed in this study.

Additional parameters can also influence the isotopic composition of biogenic carbonates and the reconstructed paleotemperatures. First, Δ_{47} reordering can significantly alter temperature estimates under conditions of deep burial or prolonged heating (e.g., Passey and Henkes, 2012; Stolper and Eiler, 2015). We consider such effects to be negligible for our material. As Cenozoic deposits in the Paris Basin are exceptionally thin, with a maximum burial depth of less than 100 m (Briais, 2015), the thermal regime experienced by the aragonitic shells remained far below thresholds known to induce measurable Δ_{47} reordering. Furthermore, the preservation of aragonite in our samples and the absence of diagenetic indicators support minimal post-depositional alteration. Consequently, we are confident that solid-state reordering did not influence our reconstructed temperatures.

Moreover, evaporation can affect the isotopic composition of shallow-water carbonates. However, Δ_{47} thermometry is insensitive to variations in water $\delta^{18}O$ associated with evaporative processes. In the studied outcrops, sedimentological evidence indicates that the fossil-bearing intervals analyzed here were not deposited under strongly evaporative conditions, limiting the potential impact of evaporation on the reconstructed temperatures (Aguerre-Chariol, 2023).

Then,the temperature obtained from clumped isotope analysis is inserted into Eq. (1) to solve for $\delta^{18}O_w$ for each Formation. Once $\delta^{18}O_w$ is constrained, high-resolution temperature reconstructions can be derived from the $\delta^{18}O$ values measured along the growth axis of each shell, using Eq. (1) from (Grossman and Ku, 1986).In addition to temperature, seawater characteristics such as paleo-salinity were estimated using the equation developed by (Pierre, 1999) for the modern Mediterranean Sea, which was considered a reasonable analogue for the Bartonian marine environment of the Paris Basin (Pomerol, 1965):

$$S = \left(\delta^{18}O_w + 8.2\right)/0.25 \quad (3)$$

where S is salinity in parts per thousand (‰), and $\delta^{18}Ow$ is expressed in ‰ relative to VSMOW.

4. Results

The evolution of the stable isotopic profiles of the shells are presented on Fig. 3. The stable isotopic profiles of the three mollusk species reveal periodic fluctuations, which can be interpreted as reflecting seasonal variations in environmental parameters, including temperature (Fig. 2).

The $\delta^{18}O$ values ranged from −1.2 ‰ to −4.5 ‰ for the *Turritelles* of

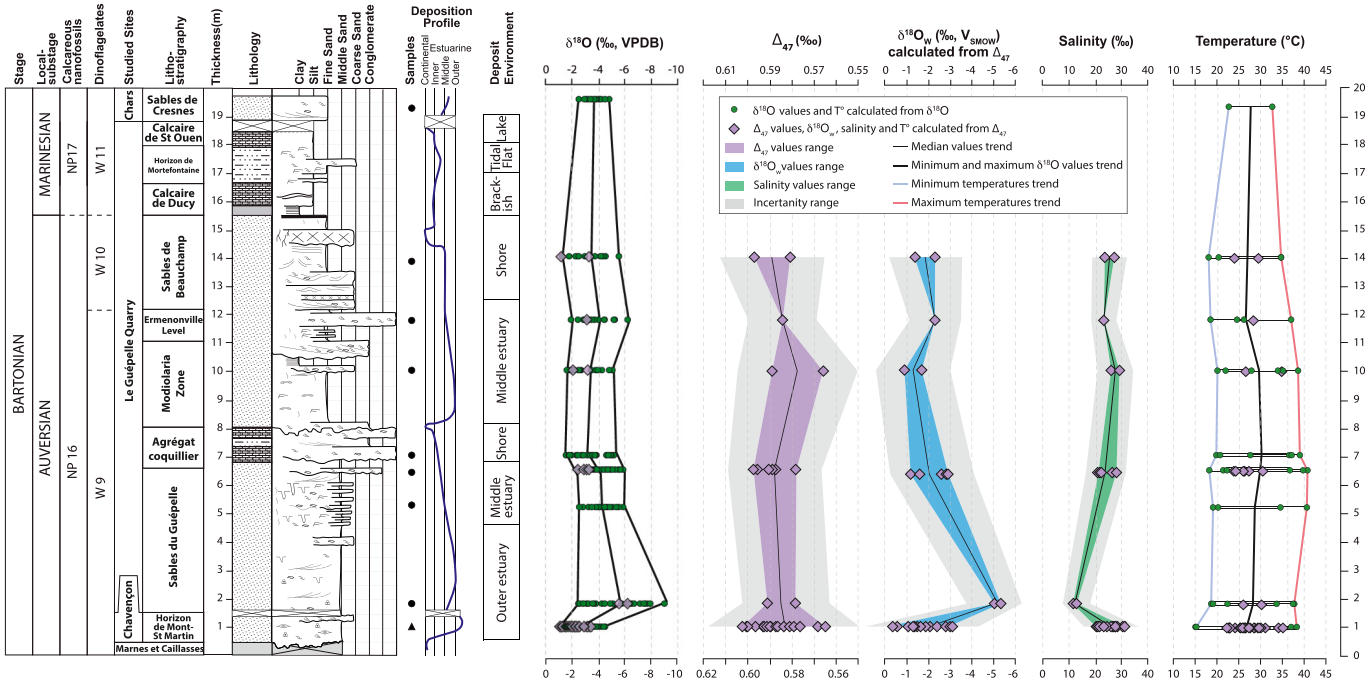

Fig. 3. Composite sedimentary succession of the Bartonian deposits in the Paris Basin, from the studied sites of Chavençon, Le Guépelle and Chars, with the local formations encountered and their associated biozones (Aubry, 1986; Briais, 2015). From left to right are represented the sedimentary deposit profile, the $\delta^{18}O$ values of *T. sulcifera*, *B. gallica* and *O. porulosum*, the Δ_{47}, $\delta^{18}O_w$ and salinity calculated from Δ_{47} and the calibrated temperatures. The white dots correspond to high resolution $\delta^{18}O$ analyses and the purple diamonds correspond to the $\delta^{18}O$ values obtained during clumped isotope analysis. (For interpretation of the references to colour in this figure legend, the reader is referred to the web version of this article.)

the Horizon de Mont Saint Martin (HMSM) at Chavençon, from −1.2 ‰ to −8.9 ‰ for the *B. gallica* across the section of le Guépelle and from −2.5 ‰ to −4.8 ‰ for the *O. porulosum* of the Sables de Cresnes Fm (Fig. 3). The highest $\delta^{18}O$ values for all shells from the Sables du Guépelle Fm shells remained consistently around −2.5 ‰, then increased to −1.5 ‰ in the Agrégat coquillier Fm and stabilized between −1.9 ‰ and − 1.2 ‰ until the Sables de Beauchamp Fm. The most negative values of the *B. gallica* first strongly increased from −8.9 ‰ in the base of the Sables du Guépelle Fm to −5.8 ‰ in the rest of this formation. The $\delta^{18}O$ then increased to −5.2 ‰ in the Agrégat coquillier Fm and − 5.0 ‰ in the Modiolaria zone. Finally, these values decreased to reach −6.2 ‰ in the Ermenonville Fm and − 5.5 ‰ in the Sables de Beauchamp Fm.

Clumped isotope analyses have been performed on the Bartonian species *T. sulcifera* and *B. gallica*. Specimens of the Sables de Cresnes Fm were too small to perform Δ_{47} measurements. Δ_{47} values were converted to temperature values using Eq. (1) from Peral et al. (2018) (Fig. 3).

Seawater $\delta^{18}O_w$ values were calculated using estimated

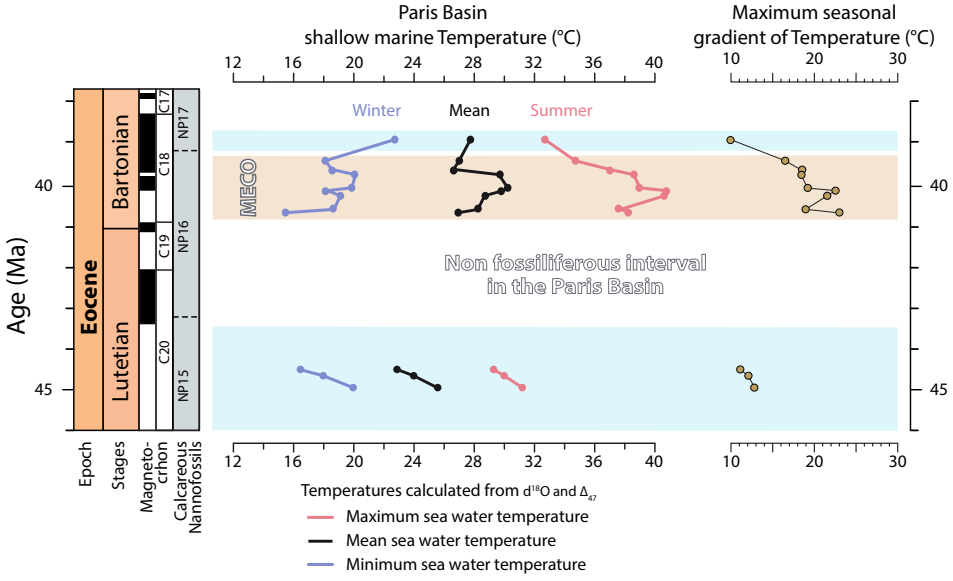

Fig. 4. Evolution of the Paris Basin littoral temperatures obtained from this study and previous works for the Lutetian from (Andreasson and Schmitz, 1996; Huyghe et al., 2012a; De Winter et al., 2020); and the seasonal gradient of temperature calculated from the difference between the extremum temperatures of the mollusks analyzed for over the Middle Eocene. Age and calcareous nannofossils zonation are from Gradstein et al. (2012).

temperatures from clumped isotopes analysis and the equation of Grossman and Ku (1986) (see methods). These values ranged from −0.9 ‰ ± 1.3 ‰ to −3.1 ‰ ± 1.2 ‰ along the Le Guépelle section except for one sample at the bottom of Le Guépelle section, which exhibited the most negative $\delta^{18}O_w$ values of −5 ‰ and − 5.3 ‰ ± 1.3 ‰ (Fig. 3). Here, because the $\delta^{18}O_w$ has been constrained by clumped isotope analyses, the Eq. (3) (Pierre, 1999) is used to calculate local salinity values. Salinity ranged from 20.4 ± 4.8 ‰ to 31.2 ± 4.8 ‰ for the HMSM and from 11.6 ± 3.6 ‰ to 29.2 ± 5.2 ‰ for Le Guépelle section (Fig. 4). Despite this broad range, the salinity at Le Guépelle remains quite stable around 25 ‰, except for one shell at the bottom of the section with a low salinity of 12 ‰, which could be explained by transient strong freshwater discharge or a transport of this specimen from a lower salinity region of the estuary.

The reconstructed temperatures fluctuate throughout the Middle Eocene in the Paris Basin (Fig. 3). Maximum annual temperatures increase from 32 ± 2 °C in the HMSM to maximum of 41 ± 5 °C at the top of the Sables du Guépelle and Agrégat Coquiller Fms. Minimum annual temperatures increased from 12 ± 3 °C to 19 ± 2 °C over the same interval before decreasing toward the top of the section.

5. Discussion

5.1. Stratigraphic position of the MECO in the Paris Basin

During the early Bartonian, the evolution of Earth temperature was characterized by a global transient warming lasting 500 kyrs (from ~40.5 to ~40 My) and corresponding to the Middle Eocene Climatic Optimum (MECO) (Fig. 3) (Bohaty et al., 2009; Bohaty and Zachos, 2003). In the oceanic record, this warming occurred within magnetochron C18n.2n (Bohaty et al., 2009; Westerhold et al., 2020). In the Paris Basin, magnetostratigraphy is infeasible due to the insufficient consolidation of the sedimentary facies, complicating correlations with oceanic records. The Sables du Guépelle Fm and its lateral equivalent, the Sables d'Auvers (Morellet and Morellet, 1948; Pomerol, 1965) have been attributed to the base of the Bartonian according to biostratigraphic and sequential evidences and more specifically to the top part of the calcareous nannofossils zone NP16 (Fig. 3) (Aubry, 1986; Gély and Lorenz, 1991). The interval with the maximum warming identified within the Bartonian composite section in the Paris Basin is located within Zone NP16 (Fig. 3), which is contemporaneous to magnetochron C18n.2n (Gradstein et al., 2020). Thus, we infer that the temperature increase observed within the Sables du Guépelle Fm corresponds to the MECO. It was not possible to point the onset of the MECO, marked by the so called pre-MECO cooling interval (Bohaty et al., 2009), because of the lack of potentially analysable fossils below the HMSM, in the Marnes et Caillasses Fm. However, the sampled shell from the Modiolaria zone seemed to mark the end of the peak of the MECO as temperatures continuously decreased above this stratigraphic level (Fig. 3).

Previous studies achieved in the Paris Basin have proposed varying stratigraphic positions for the MECO, ranging between the Sables d'Auvers Fm (Brachert et al., 2022; Kniest et al., 2024) and the Sables de Cresnes Fm (Dawber et al., 2011; Huyghe et al., 2015). These differences could be explained, for the Hampshire basin case, by a quite sparse biostratigraphic resolution concerning the lower Bartonian and the difficulty to make reliable correlation within the Paris Basin stratigraphy and with nearby basins due to important lateral facies variations (Aubry, 1985; Briais, 2015; Morellet and Morellet, 1948; Pomerol, 1965). The discrepancy with the MECO position reported by Huyghe et al. (2015) within the Sables de Cresnes Fm (NP 17), may stem from the samples' origin in historical collections, which lack precise stratigraphic control. Most likely, this study relied solely on $\delta^{18}O$ interpretations, with high uncertainty on the $\delta^{18}O_w$ constraint, potentially leading to errors in reconstructed temperature estimates and subsequent correlations with the oceanic record. Based on our results, we propose a more precise positioning of the MECO peak within the Sables du Guépelle, Sables d'Auvers, and Modiolaria zone (NP16 zone).

This refinement provides a robust chemo-stratigraphic framework across the entire climatic event, enhancing the stratigraphic resolution for the Paris Basin with a precise stratigraphic location of the MECO, compared to previous studies that investigated this event in this area (Brachert et al., 2022; Dawber et al., 2011; Huyghe et al., 2015; Kniest et al., 2024).

5.2. Expression of the MECO in the Paris Basin

The reconstructed temperatures fluctuate throughout the Middle Eocene in the Paris Basin (Fig. 4). Maximum annual temperatures first increase from 38 ± 2 °C in the HMSM to maximum of 41 ± 5 °C at the top of the Sables du Guépelle and Agrégat coquillier Fms, while minimum annual temperatures rise from 15 ± 3 °C to 19 ± 2 °C over the same interval. Summer temperatures then decrease to the top of the Guépelle section (34 ± 3 °C) whereas winter temperatures remained stable around 18 ± 3 °C.

Our results provide new insights into the expression of the MECO in shallow-water environments. Fig. 4 reports the seasonal variations in littoral seawater temperatures during the Middle Eocene in the Paris Basin. Lutetian littoral temperatures are derived from the analyses of turritellid gastropods (*Haustator imbricatarius*) and the giant gastropod *Campanile giganteum*, as reported by Andreasson and Schmitz (1996), Huyghe et al. (2012a) and De Winter et al. (2020).

Summer temperatures increased from the Lutetian, peaking at the base of the HMSM to the Agrégat coquillier Fm before undergoing a continuous decline until the end of the studied interval. Temperatures during the colder months did not mirror the summer warming trend and instead remained relatively stable throughout the Middle Eocene. This disparity between summer and winter temperature trends resulted in a significant increase in the seasonal temperature gradient shifting from 11 to 13 °C during the Lutetian to a maximum of 22–23 °C during the warming peak. The seasonal gradient then decreased gradually to the Sables de Beauchamp Fm and returning to pre-MECO values in the Sables de Cresnes Fm but should be treated with caution as no clumped isotopes measurements were done and only one specimen was analyzed.

Our results diverge from previous studies about the MECO that used corals (Brachert et al., 2022), and one bivalve (Kniest et al., 2024) from the Bartonian deposits of the Paris Basin. Both studies reconstructed a reduced seasonal thermal gradient of 7–8 °C and a wetter summer climate during the MECO. These two works present very interesting results but are subject to discussions according to their approach and by comparison to our results. Indeed, the reason for this discrepancy remains open to discussion but may partly arise from the use of collection-derived fossil specimens, which lack precise stratigraphic positioning within the Le Guépelle and Caumont sections, unlike the material analyzed in our study. Moreover, Brachert et al. (2022), provided a high-resolution reconstruction of the seasonal temperature gradient using corals, whereas our study is based on mollusks.

. Their reconstructions relied in several key assumptions, particularly that the $\delta^{18}O_w$ remained constant throughout the year. In contrast, our results indicate that this parameter varied between winter and summer (Fig. 3), suggesting that previous studies may have underestimated the seasonal temperature gradient during this interval. Regarding Kniest et al. (2024), only a single collection-derived fossil was analyzed, which introduces both stratigraphic uncertainties and neglects potential temperature fluctuations at meteorological timescales.

In this regard, our results, which indicate a pronounced seasonal temperature gradient and peak precipitation during winter, show better agreement with climate model simulations for the mid-Eocene (Baatsen et al., 2020; Li et al., 2022).

5.3. Implication for the climate of the Paris Basin during the MECO

Understanding the impact of an hyperthermal event on the

hydrologic system is also of primary importance (Chen et al., 2018; Peris Cabré et al., 2023). We addressed this question throughout the fluctuations of the $\delta^{18}O_w$ and seawater salinity in function of temperature, i.e. the season of the year. We report the $\delta^{18}O_w$ values of seawater in the Paris Basin as a function of temperature derived from Δ_{47} values on Fig. 5. In shallow-water environments, salinity values can be inferred directly from $\delta^{18}O_w$ values and our dataset reveals a strong correlation between these parameters. This relationship highlights distinct seasonal variations in salinity, with elevated values (~30 psu) during the warmest months and significantly lower salinity (~25 to 20 psu) during colder months. Only one sample, that shows very reduced salinities (between 10 and 15 psu) deviates from of this correlation (Fig. 5). This sample was possibly exported from an inner part of the estuary or corresponded to a period of very important river discharge.

We present on Fig. 6 a paleoenvironmental reconstruction for winter and summer periods of the Paris Basin during the MECO, integrating the hydrologic system. Under the warm climatic conditions of the Middle Eocene, the seasonal ratio between evaporation and precipitations probably played a critical role in shaping salinity dynamics within the Paris Basin estuary, even if it has been demonstrated on modern estuaries of Florida that precipitations play a major impact than evaporation on this parameter (Summer and Belaineh, 2005). Thus, during summer, increased evaporation likely increased salinity. Conversely, the low salinity observed during colder periods may particularly reflect a seasonal influx of freshwater, possibly driven by enhanced precipitation and runoff during winter months, as observed in tropical modern estuaries (Summer and Belaineh, 2005). The interplay between these processes is further contextualized by the paleogeography of the Paris Basin during the Middle Eocene (Figs. 1 and 6). These findings agree with modelling results arguing for strongly monsoonal climate at this period (Baatsen et al., 2020).

Our results provide a detailed characterization of the climate in the Paris Basin during the MECO. Based on the reconstructed seasonal temperature gradient (~20 °C) and evidence of warm summers coupled with a rainy winter season, the climate aligns with the characteristics of a hot summer Mediterranean climate, according to Köppen's classification. However, contemporary Mediterranean climates typically exhibit maximum mean summer temperatures of ~30 °C. In contrast, our reconstructions suggest that seawater temperatures in the Paris Basin during the MECO may have reached extreme values of up to ~40 °C during the warmest months, consistent with higher pCO_2 levels (~1000 ppm) during the Middle Eocene (Hönisch et al., 2023).

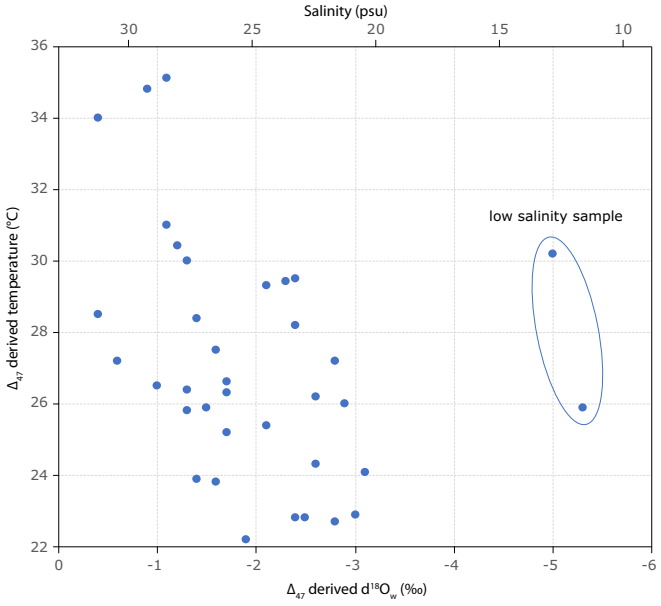

Fig. 5. Correlation graph between the temperatures calculated directly from Δ_{47} measurements with $\delta^{18}O_w$ values also calculated from Δ_{47} measurements. Salinity is calculated from $\delta^{18}O_w$ values following the equation of Pierre (1999) for the modern Mediterranean Sea.

This reconstructed thermal regime significantly exceeds the thresholds observed in present-day Mediterranean climate type, leading us to propose that the Paris Basin experienced a "super-hot summer Mediterranean climate" during the MECO. Such a climatic state would have been marked by unprecedented summer heat, likely resulting from amplified greenhouse forcing and elevated atmospheric CO_2 concentrations characteristic of hyperthermal events. This climatic configuration underscores the regional amplification of global warming signals during hyperthermal events, particularly in mid-latitude basins like the Paris Basin.

The asymmetrical pattern of freshwater input and rainfall identified from our results agrees with numerical models that also demonstrate higher precipitations during winter in western Europe, reflecting a monsoonal trend (Baatsen et al., 2020; Li et al., 2022).

5.4. *Expression of the MECO and implications for the future*

Fig. 7 presents a comparison in the climatic evolution between the Paris Basin and the oceanic domain. In the oceanic realm, the MECO led to a 4–6 °C rise in deep and sea-surface temperatures (Bijl et al., 2010; Bohaty et al., 2009; Bohaty and Zachos, 2003; Cramwinckel et al., 2018; Sluijs et al., 2013), with peak temperatures reaching 33 °C in the eastern equatorial Atlantic Ocean (Cramwinckel et al., 2018) and 28 °C in the eastern Tasmanian Plateau (Bijl et al., 2010; Bijl et al., 2009). In contrast, shallow-water temperatures in the Paris Basin peaked at 41 °C. This can appear extreme, but this apparent intensification might likely be accentuated by the reduced water column thickness at the Agrégat coquillier Fm., where extremely shallow conditions promote enhanced surface water warming (Aguerre-Chariol, 2023). Furthermore, the pattern of global oceanic temperature increase mirrors that of mean annual and summer temperatures in the Paris Basin, lacking the climatic pattern during cold months. Our results emphasize the importance of integrating shallow-marine records with global datasets to better understand the spatial and temporal complexity of these hyperthermal events.

Concerning the continental domain, Δ_{47} analyses of lacustrine and paleosol sediments of North-West America indicates a mean annual warming of 9 °C during the MECO (Methner et al., 2016). The climate went from hot and semi / sub-humid during the MECO to dry and cold during the post MECO cool in North-West America and the seasonal gradient seem stronger during the MECO than after (Mulch et al., 2015)., suggesting similar trends compared to the Paris Basin.

The evolution of future seasonality in the context of global warming remains uncertain and depends on the climate model used. Most studies agree on a significant rise in summer temperature, but projections for winter temperatures vary. Recent works suggest that European winter temperatures will increase during the 21th century (Carvalho et al., 2021). In contrast, other models indicate that tropical winter SST may decrease slightly due to stronger winter tropical wind (Sobel and Camargo, 2011). Our results show that during the MECO hyperthermal event in mid-latitudes, where tropical climate prevailed, only warm-season temperatures increased significantly, while colder-month temperatures remained stable, confirming a stronger summer response to global warming and relatively stable winter temperatures in these areas.

6. Conclusions

This study presents a high-resolution reconstruction of seasonal seawater temperatures in the Paris Basin during the Middle Eocene Climatic Optimum (MECO), using $\delta^{18}O$ and Δ_{47} analyses of shallow-marine mollusks. Our results reveal a substantial amplification of seasonal temperature variability, with summer temperatures rising by up to

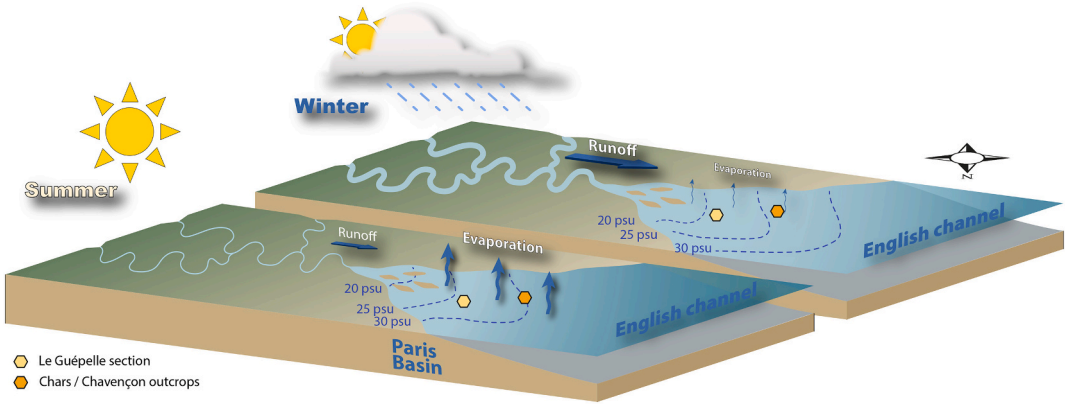

Fig. 6. Simplified 3D diagrams illustrating the hydrological system of the Paris Basin during the MECO. During the summer period, the temperature is high, rainfall is reduced, and evaporation is elevated, implying normal salinity in the estuary. In winter, temperature and evaporation decrease, while rainfall and runoff increase, thus decreasing salinity in the coastal environments of the basin.

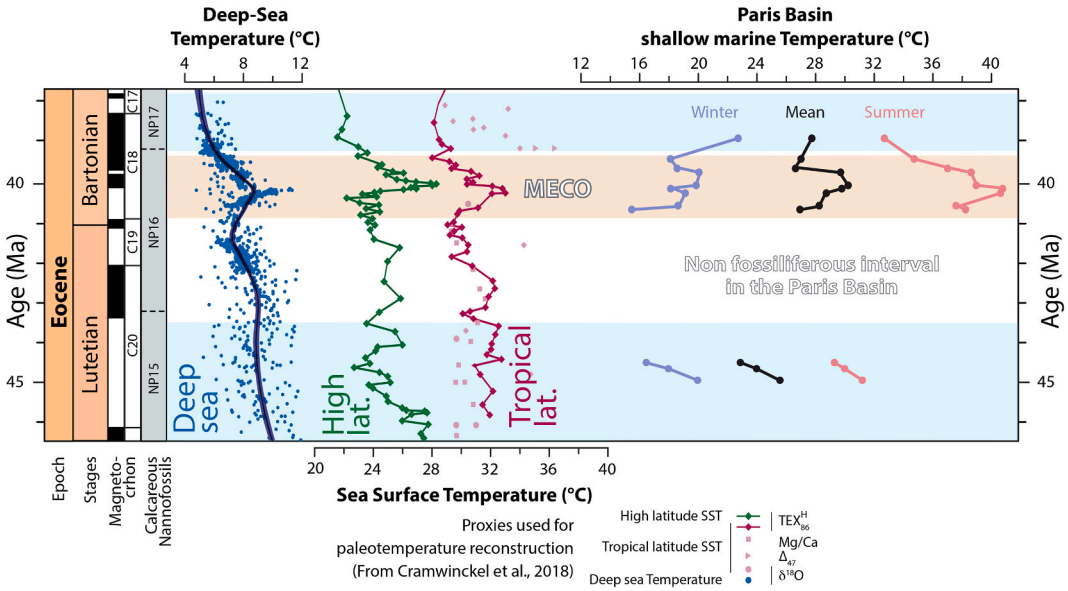

Fig. 7. Compilation of oceanic deep-sea and sea surface temperatures obtain by various proxies over the Middle Eocene (Cramwinckel et al., 2018) and Paris Basin littoral temperatures obtained from this study and previous works for the Lutetian from (Andreasson and Schmitz, 1996; Huyghe et al., 2012b; De Winter et al., 2020) over the Middle Eocene. Age and calcareous nannofossils zonation are from Gradstein et al. (2012).

10 °C, while winter temperatures remained relatively stable. This seasonal asymmetry led to a pronounced rise in thermal seasonality, reaching a maximum of ~22 °C.

Peak summer temperatures approached 41 °C, suggesting the Paris Basin experienced an extreme form of Mediterranean climate, consistent with contemporaneous elevated atmospheric pCO_2 concentrations. Additionally, reconstructed seawater $\delta^{18}O$ and salinity values highlight a seasonal hydrological cycle dominated by evaporation during dry summers and enhanced freshwater influx during wetter winters, consistent with a monsoonal-like climate regime.

These findings improve the stratigraphic resolution of the middle Eocene within the Paris Basin from chemostratigraphic evidence. It also underscores the importance of incorporating shallow-marine records into global paleoclimatic reconstructions. The reconstructed climate offers an informative analogue for future climate scenarios under continued anthropogenic warming, particularly for regions currently experiencing Mediterranean-like climates.

Supplementary data to this article can be found online at https://doi.org/10.1016/j.palaeo.2026.113547.

CRediT authorship contribution statement

Loïc Marlot: Writing – original draft, Formal analysis, Data curation, Conceptualization. **Damien Huyghe:** Writing – original draft, Validation, Supervision, Project administration, Funding acquisition, Formal analysis, Data curation, Conceptualization. **Justine Briais:** Writing – original draft, Validation, Supervision, Project administration, Funding acquisition, Data curation, Conceptualization. **Mathieu Daëron:** Writing – original draft, Supervision, Methodology, Formal analysis. **Christine Flehoc:** Writing – original draft, Validation, Supervision, Methodology, Conceptualization. **Laurent Emmanuel:** Writing – original draft, Validation, Methodology. **Didier Merle:** Writing – original draft, Validation, Methodology, Data curation. **Olivier Aguerre-Charriol:** Writing – original draft, Validation, Formal analysis, Data curation. **Franck Lartaud:** Writing – original draft, Validation, Supervision, Funding acquisition, Data curation.

Declaration of competing interest

The authors declare no conflict of interest.

Acknowledgements

The authors would like to thank the RGF (Référentiel Géologique de la France) and the CNRS for their support through the MITI interdisciplinary program *Le Temps* (ARCHIVE), which funded this study. This research was further supported by a PhD grant from the French Ministry of Industry and the BRGM (Bureau de Recherches Géologiques et Minières) awarded to Loïc Marlot. We are also grateful to the Conseil Départemental du Val-d'Oise for granting us access to the protected site of Le Guepelle. Finally, we would like to express our thanks to Nicolas Seigneur and Léo Szewczyk for their valuable proofreading of this article. The authors also thank Editor Bing Shen and two anonymous reviewers for their constructive comments, which helped improve the manuscript.

Data availability

The authors confirm that all data necessary for supporting the scientific findings of this paper have been provided.

References

Aguerre-Chariol, O., 2023. Stratigraphie, sédimentologie et paléoenvironnements dans le site du Guépelle (Saint-Witz, Val d'Oise). Bull. Inf. Géol. Bassin Paris 60 (3), 3–32.

Allmon, W.D., 1988. Ecology of recent Turritellina Gastropods (Prosobranchia, Turritellidae): current knowledge and paleontological implications. Palaios 3, 259–284.

Andreasson, F.P., Schmitz, B., 1996. Winter and summer temperatures of the early middle Eocene of France from Turritella $\delta^{18}O$ profiles. Geology 24 (12), 1067–1070.

Andreasson, F.P., Schmitz, B., 2000. Temperature seasonality in the early middle Eocene North Atlantic region: evidence from stable isotope profiles of marine gastropod shells. Geol. Soc. Am. Bull. 112 (4), 628–640.

Aubry, M.-P., 1985. Northwestern European Paleogene magnetostratigraphy, biostratigraphy, and paleogeography: Calcareous nannofossil evidence. Geology 13 (3), 198–202.

Aubry, M.-P., 1986. Paleogene calcareous nannoplankton biostratigraphy of northwestern Europe. Palaeogeogr. Palaeoclimatol. Palaeoecol. 55, 267–334.

Baatsen, M., Von Der Heydt, A.S., Huber, M., Kliphuis, M.A., Bijl, P.K., Sluijs, A., Dijkstra, H.A., 2020. The middle to late Eocene greenhouse climate modelled using the CESM 1.0.5. Clim. Past 16, 2573–2597.

Barbin, V., 2013. Application of cathodoluminescence microscopy to recent and past biological materials: a decade of progress. Mineral. Petrol. 107, 353–362.

Bernasconi, S.M., Müller, I.A., Bergmann, K.D., Breitenbach, S.F.M., Fernandez, A., Hodell, D.A., Jaggi, M., Meckler, A.N., Millan, I., Ziegler, M., 2018. Reducing uncertainties in carbonate clumped isotope analysis through consistent carbonate-based standardization. Geochem. Geophys. Geosyst. 19, 2895–2914.

Bernasconi, S.M., Daëron, M., Bergmann, K.D., Bonifacie, M., Meckler, A.N., Affek, H.P., Anderson, N., Bajnai, D., Barkan, E., Beverly, E., Blamart, D., Burgener, L., Calmels, D., Chaduteau, C., Clog, M., Davidheiser-Kroll, B., Davies, A., Dux, F., Eiler, J., Elliott, B., Fetrow, A.C., Fiebig, J., Goldberg, S., Hermoso, M., Huntington, K.W., Hyland, E., Ingalls, M., Jaggi, M., John, C.M., Jost, A.B., Katz, S., Kelson, J., Kluge, T., Kocken, I.J., Laskar, A., Leutert, T.J., Liang, D., Lucarelli, J., Mackey, T.J., Mangenot, X., Meinicke, N., Modestou, S.E., Müller, I.A., Murray, S., Neary, A., Packard, N., Passey, B.H., Pelletier, E., Petersen, S., Piasecki, A., Schauer, A., Snell, K.E., Swart, P.K., Tripati, A., Upadhyay, D., Vennemann, T., Winkelstern, I., Yarian, D., Yoshida, N., Zhang, N., Ziegler, M., 2021. InterCarb: a community effort to improve interlaboratory standardization of the carbonate clumped isotope thermometer using carbonate standards. Geochem. Geophys. Geosyst. 22 (5), e2020GC009588.

Bijl, P.K., Schouten, S., Sluijs, A., Reichart, G.-J., Zachos, J.C., Brinkhuis, H., 2009. Early Palaeogene temperature evolution of the Southwest Pacific Ocean. Nature 461, 776–779.

Bijl, P.K., Houben, A.J.P., Schouten, S., Bohaty, S.M., Sluijs, A., Reichart, G.-J., Sinninghe Damsté, J.S., Brinkhuis, H., 2010. Transient Middle eocene atmospheric CO_2 and temperature variations. Science 330, 819–821.

Bijl, P.K., Pross, J., Warnaar, J., Stickley, C.E., Huber, M., Guerstein, R., Houben, A.J.P., Sluijs, A., Visscher, H., Brinkhuis, H., 2011. Environmental forcings of Paleogene Southern Ocean dinoflagellate biogeography. Paleoceanography 26 (1).

Bohaty, S.M., Zachos, J.C., 2003. Significant Southern Ocean warming event in the late middle Eocene. Geology 31, 1017–1020.

Bohaty, S.M., Zachos, J.C., Florindo, F., Delaney, M.L., 2009. Coupled greenhouse warming and deep-sea acidification in the middle Eocene: Middle Ecoene warming and CCD shoaling. Paleoceanography 24 (2).

Bonifacie, M., Calmels, D., Eiler, J.M., Horita, J., Chaduteau, C., Vasconcelos, C., Agrinier, P., Katz, A., Passey, B.H., Ferry, J.M., Bourrand, J.J., 2017. Calibration of the dolomite clumped isotope thermometer from 25 to 350 C, and implications for a universal calibration for all (Ca, Mg, Fe) CO_3 carbonates. Geochim. Cosmochim. Acta 200, 255–279.

Boscolo Galazzo, F., Thomas, E., Giusberti, L., 2015. Benthic foraminiferal response to the Middle Eocene Climatic Optimum (MECO) in the South-Eastern Atlantic (ODP Site 1263). Palaeogeogr. Palaeoclimatol. Palaeoecol. 417, 432–444.

Brachert, T.C., Felis, T., Gagnaison, C., Hoehle, M., Reuter, M., Spreter, P.M., 2022. Slow-growing reef corals as climate archives: a case study of the Middle Eocene Climatic Optimum 40 Ma ago. Sci. Adv. 8 (20), eabm3875.

Brachert, T.C., Agnini, C., Gagnaison, C., Gély, J.-P., Henehan, M.J., Westerhold, T., 2023. Astronomical pacing of middle eocene sea-level fluctuations: inferences from shallow-water carbonate ramp deposits. Paleoceanogr. Paleoclimatol. 38, e2023PA004633.

Brand, W.A., Assonov, S.S., Coplen, T.B., 2010. Correction for the ^{17}O interference in $\delta(13C)$ measurements when analyzing CO_2 with stable isotope mass spectrometry (IUPAC Technical Report). Pure Appl. Chem. 82 (8), 1719–1733. https://doi.org/10.1351/PAC-REP-09-01-05.

Briais, J., 2015. Le Cénozoïque du bassin de Paris: un enregistrement sédimentaire haute résolution des déformations lithosphériques en régime de faible subsidence (Thèse). Université Rennes 1, Rennes.

Burke, K.D., Williams, J.W., Chandler, M.A., Haywood, A.M., Lunt, D.J., Otto-Bliesner, B. L., 2018. Pliocene and Eocene provide best analogs for near-future climates. Proc. Natl. Acad. Sci. 115 (52), 13288–13293.

Carvalho, D., Cardoso Pereira, S., Rocha, A., 2021. Future surface temperatures over Europe according to CMIP6 climate projections: an analysis with original and bias-corrected data. Clim. Chang. 167 (1), 10.

Cavelier, C., Pomerol, C., 1979. Chronologie et interpretation des evenements tectoniques cenozoiques dans le Bassin de Paris. Bulletin de la Société Géologique de France 7 (1), 22–48.

Chen, C., Guerit, L., Foreman, B.Z., Hassenruck-Gudipati, H.J., Adatte, T., Honegger, L., Perret, M., Sluijs, A., Castelltort, S., 2018. Estimating regional flood discharge during Palaeocene-Eocene global warming. Sci. Rep. 8, 13391.

Cramwinckel, M.J., Huber, M., Kocken, I.J., Agnini, C., Bijl, P.K., Bohaty, S.M., Frieling, J., Goldner, A., Hilgen, F.J., Kip, E.L., Peterse, F., van der Ploeg, R., Röhl, U., Schouten, S., Sluijs, A., 2018. Synchronous tropical and polar temperature evolution in the Eocene. Nature 559, 382–386.

Daëron, M., 2021. Full propagation of analytical uncertainties in Δ_{47} measurements. Geochem. Geophys. Geosyst. 22, e2020GC009592.

Daëron, M., Blamart, D., Peral, M., Affek, H.P., 2016. Absolute isotopic abundance ratios and the accuracy of Δ_{47} measurements. Chem. Geol. 442, 83–96.

Daëron, M., Drysdale, R.N., Peral, M., Huyghe, D., Blamart, D., Coplen, T.B., Lartaud, F., Zanchetta, G., 2019. Most Earth-surface calcites precipitate out of isotopic equilibrium. Nat. Commun. 10, 429.

Daëron, M., Vermeesch, P., 2024. Omnivariant generalized least squares regression: Theory, geochronological applications, and making the case for reconcilied D47 calibrations. Chemical Geology 647, 121881.

Dawber, C.F., Tripati, A.K., Gale, A.S., MacNiocaill, C., Hesselbo, S.P., 2011. Glacioeustasy during the middle Eocene? Insights from the stratigraphy of the Hampshire Basin, UK. Palaeogeogr. Palaeoclimatol. Palaeoecol. 300, 84–100.

de Rafélis, M., Renard, M., Emmanuel, L., Durlet, C., 2000. Apport de la cathodoluminescence à la connaissance de la spéciation du manganèse dans les carbonates pélagiques. C. R. Acad. Sci. Ser. IIA Earth Planet. Sci. 330, 391–398.

De Winter, N.J., Vellekoop, J., Clark, A.J., Stassen, P., Speijer, R.P., Claeys, P., 2020. The Giant Marine Gastropod *Campanile Giganteum* (Lamarck, 1804) as a high-resolution archive of seasonality in the Eocene Greenhouse World. Geochem. Geophys. Geosyst. 21.

De Winter, N.J., Witbaard, R., Kocken, I.J., Müller, I.A., Guo, J., Goudsmit, B., Ziegler, M., 2022. Temperature dependence of clumped isotopes (Δ_{47}) in aragonite. Geophys. Res. Lett. 49 (20), e2022GL099479.

De Winter, N.J., Tindall, J., Johnson, A.L.A., Goudsmit-Harzevoort, B., Wichern, N., Kaskes, P., Claeys, P., Huygen, F., Van Leeuwen, S., Metcalfe, B., Bakker, P., Goolaerts, S., Wesselingh, F., Ziegler, M., 2024. Amplified seasonality in western Europe in a warmer world. Sci. Adv. 10, eadl6717.

Edgar, K.M., Bohaty, S.M., Gibbs, S.J., Sexton, P.F., Norris, R.D., Wilson, P.A., 2013. Symbiont "bleaching" in planktic foraminifera during the Middle Eocene Climatic Optimum. Geology 41, 15–18.

Eiler, J.M., 2011. Paleoclimate reconstruction using carbonate clumped isotope thermometry. Quat. Sci. Rev. 30, 3575–3588. https://doi.org/10.1016/j.quascirev.2011.09.001.

Fuksi, T., Tomašových, A., Gallmetzer, I., Haselmair, A., Zuschin, M., 2018. 20th century increase in body size of a hypoxia-tolerant bivalve documented by sediment cores from the northern Adriatic Sea (Gulf of Trieste). Mar. Pollut. Bull. 135, 361–375. https://doi.org/10.1016/j.marpolbul.2018.07.004.

Gély, J.-P., Lorenz, C., 1991. Analyse séquentielle de l'Eocène et de l'Oligocène du Bassin parisien (France). Revue de l'institut Français du Pétrole 713–747.

Gradstein, F.M., Ogg, G., Schmitz, M., Ogg, G.M., 2012. The Geologic Time Scale 2012 (Elsevier. ed).

Gradstein, F.M., Ogg, J.G., Schmitz, M.D., Ogg, G.M., 2020. The Geologic Time Scale 2020. Elsevier, Amsterdam.

Grossman, E.L., Ku, T.-L., 1986. Oxygen and carbon isotope fractionation in biogenic aragonite: Temperature effects. Chem. Geol. (Isotope Geosci. Sect.) 59, 59–74.

Guillocheau, F., Robin, C., Allemand, P., Bourquin, S., Brault, N., Dromart, G., Grandjean, G., 2000. Evolution tectonique méso-cénozoïque du bassin de Paris: contraintes stratigraphiques 3D. Geodin. Acta 13, 189–245.

He, S., Wang, T., Spicer, R.A., Farnsworth, A., Mulch, A., Widdowson, M., Zhang, Q., Cai, F., Valdes, P.J., Wang, C., Randrianaly, H.N., Xie, J., Ding, L., 2025. Back to an ice-free future: early cretaceous seasonal cycles of sea surface temperature and glacier ice. Sci. Adv. 11, eadr9417.

Henehan, M.J., Edgar, K.M., Foster, G.L., Penman, D.E., Hull, P.M., Greenop, R., Anagnostou, E., Pearson, P.N., 2020. Revisiting the Middle Eocene Climatic optimum "Carbon Cycle Conundrum" with new estimates of Atmospheric pCO $_2$ from Boron Isotopes. Paleoceanogr. Paleoclimatol. 35.
Holmes, S., Miller, N., 2006. Aspects of the ecology and population genetics of the bivalve *Corbula gibba*. Mar. Ecol. Prog. Ser. 315, 129–140.
Huyghe, D., Merle, D., Lartaud, F., Cheype, E., Emmanuel, L., 2012. Middle Lutetian climate in the Paris Basin: implications for a marine hotspot of paleobiodiversity. Facies 58 (4), 587–604.
Huyghe, D., Lartaud, F., Emmanuel, L., Merle, D., Renard, M., 2015. Palaeogene climate evolution in the Paris Basin from oxygen stable isotope ($\delta^{18}O$) compositions of marine molluscs. J. Geol. Soc. Lond. 172, 576–587.
Huyghe, D., Daëron, M., de Rafelis, M., Blamart, D., Sébilo, M., Paulet, Y.-M., Lartaud, F., 2022. Clumped isotopes in modern marine bivalves. Geochim. Cosmochim. Acta 316, 41–58.
Hönisch, B., and the, 2023. Cenozoic CO2 proxy investigation project (CECO2PIP) consortium. Toward a Cenozoic history of atmospheric CO2. Science 382 (6675), eadi5177.
Ivany, L.C., Judd, E.J., 2022. Deciphering temperature seasonality in Earth's Ancient Oceans. Annu. Rev. Earth Plan. Sci. Lett. 50, 123–152.
Jones, D.S., Allmon, W.D., 1995. Records of upwelling, seasonality and growth in stable-isotope profiles of Pliocene mollusk shells from Florida. Lethaia 28 (1), 61–74.
Kniest, J.F., Davies, A.J., Brugger, J., Fiebig, J., Bernecker, M., Todd, J.A., Hickler, T., Voigt, S., Woodland, A., Raddatz, J., 2024. Dual clumped isotopes from Mid-Eocene bivalve shell reveal a hot and summer wet climate of the Paris Basin. Commun. Earth Environ. 5 (1), 330.
Lartaud, F., Emmanuel, L., de Rafelis, M., Ropert, M., Labourdette, N., Richardson, C.A., Renard, M., 2010. A latitudinal gradient of seasonal temperature variation recorded in oyster shells from the coastal waters of France and the Netherlands. Facies 56, 13–25.
Lear, C.H., Anand, P., Blenkinsop, T., Foster, G.L., Gagen, M., Hoogakker, B., Larter, R.D., Lunt, D.J., McCave, I.N., McClymont, E., Pancost, R.D., Rickaby, R.E.M., Schultz, D. M., Summerhayes, C., Williams, C.J.R., Zalasiewicz, J., 2021. Geological Society of London Scientific Statement: what the geological record tells us about our present and future climate. J. Geol. Soc. Lond. 178 (1), jgs2020-239.
Li, X., Hu, Y., Guo, J., Lan, J., Lin, Q., Bao, X., Yuan, S., Wei, M., Li, Z., Man, K., Yin, Z., Han, J., Zhang, J., Zhu, C., Zhao, Z., Liu, Y., Yang, J., Nie, J., 2022. A high-resolution climate simulation dataset for the past 540 million years. Sci. Data 9, 371.
Marchegiano, M., John, C.M., 2022. Disentangling the impact of global and regional climate changes during the Middle Eocene in the Hampshire Basin: new insights from carbonate clumped isotopes and ostracod assemblages. Paleoceanogr. Paleoclimatol. 37 (2), e2021PA004299.
Mégnien, C., 1980. Stratigraphie et Paléontologie. In: Mégnien, C. (ed.) Synthèse Géologique du bassin de Paris, Volume 1. Mémoire du BRGM, 101, 1-466.
Merle, D., 2008. Stratotype Lutétien. Biotope 288.
Methner, K., Mulch, A., Fiebig, J., Wacker, U., Gerdes, A., Graham, S.A., Chamberlain, C. P., 2016. Rapid Middle Eocene temperature change in western North America. Earth Planet. Sci. Lett. 450, 132–139.
Mirzaei, M.R., Hosseini, S.A., 2017. Clam (Corbula modesta) as a bio-indicator of environmental condition: the case of Chabahar Bay. Res. Mar. Sci. 2, 221–227.
Moreau, K., Andrieu, S., Briais, J., Brigaud, B., Ader, M., 2024. Facies distribution and depositional cycles in lacustrine and palustrine carbonates: The Lutetian–Aquitanian record in the Paris Basin. Depositional Rec. 10, 124–158.
Morellet, L., Morellet, J., 1948. Le Bartonien du Bassin de Paris, Mémoires du Service de la Carte Géologique de la France. Imprimerie Nationale, p. 437.
Mulch, A., Chamberlain, C.P., Cosca, M.A., Teyssier, C., Methner, K., Hren, M.T., Graham, S.A., 2015. Rapid change in high-elevation precipitation patterns of western North America during the Middle Eocene Climatic Optimum (MECO). Am. J. Sci. 315, 317–336.
Passey, B.H., Henkes, G.A., 2012. Carbonate clumped isotope bond reordering and geospeedometry. Earth Planet. Sci. Lett. 351, 223–236.
Peral, M., Daëron, M., Blamart, D., Bassinot, F., Dewilde, F., Smialkowski, N., Isguder, G., Bonnin, J., Jorissen, F., Kissel, C., Michel, E., Vázquez Riveiros, N., Waelbroeck, C., 2018. Updated calibration of the clumped isotope thermometer in planktonic and benthic foraminifera. Geochim. Cosmochim. Acta 239, 1–16.
Peris Cabré, S., Valero, L., Spangenberg, J.E., Vinyoles, A., Verité, J., Adatte, T., Tremblin, M., Watkins, S., Sharma, N., Garcés, M., Puigdefàbregas, C., Castelltort, S., 2023. Fluvio-deltaic record of increased sediment transport during the Middle Eocene Climatic Optimum (MECO), Southern Pyrenees, Spain. Clim. Past 19, 533–554.
Pierre, C., 1999. The oxygen and carbon isotope distribution in the Mediterranean water masses. Mar. Geol. 153, 41–55.
Pomerol, C., 1965. Les Sables de l'Éocène supérieur (Lédien et Bartonien) des bassins de Paris et de Bruxelles. Mémoires du Service de la Carte Géologique de la France, Paris, p. 214.
Pomerol, C., 1973. Ere cénozoïque: tertiaire et quaternaire. Doin, Paris, p. 269.
Quizon, A.A., Petersen, S.V., de Winter, N.J., Vellekoop, J., 2025. Clumped isotope thermometry (Δ47) measurements in marine gastropods suggest equilibrium precipitation. Geochim. Cosmochim. Acta 410, 234–249.
Robin, C., Allemand, P., Burov, E., Doin, M.P., Guillocheau, F., Dromart, G., Garcia, J.-P., 2003. Vertical movements of the Paris Basin (Triassic-Pleistocene): from 3D stratigraphic database to numerical models. Geol. Soc. Lond. Spec. Publ. 212, 225–250.
Schlidt, V., Evans, D., de Winter, N.J., Bernecker, M., Arndt, I., Staudigel, P.T., Davies, A. J., Brand, U., Müller, W., Fiebig, J., 2025. Most bivalves and gastropods calcify indistinguishably from dual clumped isotope equilibrium. Geochim. Cosmochim. Acta 410, 174–187.
Scholz, S.R., Petersen, S.V., Escobar, J., Jaramillo, C., Hendy, A.J., Allmon, W.D., Curtis, J.H., Anderson, B., Hoyos, N., Restrepo, J.C., Perez, N., 2020. Isotope sclerochronology indicates enhanced seasonal precipitation in northern South America (Colombia) during the Mid-Miocene Climatic Optimum. Geology 48 (7), 668–672.
Scholz, S.R., Petersen, S.V., Anderson, B.M., 2024. Modern reconstructions of mean and seasonal-scale climate from coastal marine gastropods (Turritellidae). Palaeogeogr. Palaeoclimatol. Palaeoecol. 655, 112553.
Sluijs, A., Zeebe, R.E., Bijl, P.K., Bohaty, S.M., 2013. A middle Eocene carbon cycle conundrum. Nat. Geosci. 6, 429–434.
Sobel, A.H., Camargo, S.J., 2011. Projected future seasonal changes in tropical summer climate. J. Clim. 24, 473–487.
Stolper, D.A., Eiler, J.M., 2015. The kinetics of solid-state isotope-exchange reactions for clumped isotopes: a study of inorganic calcites and apatites from natural and experimental samples. Am. J. Sci. 315 (5), 363–411.
Summer, D.N., Belaineh, G., 2005. Evaporation, Precipitation, and Associated Salinity Changes at a Humid, Subtropical Estuary. Estuaries, pp. 844–855.
Tierney, J.E., Poulsen, C.J., Montañez, I.P., Bhattacharya, T., Feng, R., Ford, H.L., Hönisch, B., Inglis, G.N., Petersen, S.V., Sagoo, N., Tabor, C.R., Thirumalai, K., Zhu, J., Burls, N.J., Foster, G.L., Goddéris, Y., Huber, B.T., Ivany, L.C., Kirtland Turner, S., Lunt, D.J., McElwain, J.C., Mills, B.J.W., Otto-Bliesner, B.L., Ridgwell, A., Zhang, Y.G., 2020. Past climates inform our future. Science 370, eaay3701.
Wefer, G., Berger, W.H., 1991. Isotope paleontology: growth and composition of extant calcareous species. Mar. Geol. 100 (1–4), 207–248.
Westerhold, T., Marwan, N., Drury, A.J., Liebrand, D., Agnini, C., Anagnostou, E., Barnet, J.S.K., Bohaty, S.M., De Vleeschouwer, D., Florindo, F., Frederichs, T., Hodell, D.A., Holbourn, A.E., Kroon, D., Lauretano, V., Littler, K., Lourens, L.J., Lyle, M., Pälike, H., Röhl, U., Tian, J., Wilkens, R.H., Wilson, P.A., Zachos, J.C., 2020. An astronomically dated record of Earth's climate and its predictability over the last 66 million years. Science 369, 1383–1387.
Wisshak, M., Neumann, C., Jakobsen, J., Freiwald, A., 2009. The 'living-fossil community'of the cyrtocrinid Cyathidium foresti and the deep-sea oyster Neopycnodonte zibrowii (Azores Archipelago). Palaeogeogr. Palaeoclimatol. Palaeoecol. 271 (1–2), 77–83.
Zachos, J., Pagani, M., Sloan, L., Thomas, E., Billups, K., 2001. Trends, rhythms, and aberrations in global climate 65 Ma to present. Science 292, 686–693.